Mon. Not. R. Astron. Soc. **284,** 773–784 (1997)

Molecular gas in polar-ring galaxies

G. Galletta,[1] L. J. Sage[2] and L. S. Sparke[3]

[1]*Dipartimento di Astronomia, Università di Padova, I 35122 Padova, Italy*
[2]*Department of Astronomy, University of Maryland, College Park MD 20742, USA*
[3]*Department of Astronomy, University of Wisconsin, Madison WI, USA*

Accepted 1996 September 22. Received 1996 July 10

ABSTRACT

We present CO $J=1\rightarrow0$ observations ($\lambda=2.6$ mm) of 10 polar-ring galaxies, chosen from the Polar Ring Catalogue; we infer masses of H_2 ranging from 7×10^7 to $2\times10^{10}\,M_\odot$, with an average of about $1\times10^9\,M_\odot$. These H_2 masses are greater than the average molecular mass of an early-type galaxy; we previously found similar results for a sample of minor-axis dust-lane ellipticals. In the cases where we can estimate the gas mass in the polar ring, including the H I masses from literature, they are high enough to allow self-gravitation to stabilize the rings. This means that the ages of the rings may be ≥1 Gyr. Indeed, the gas masses are often greater than those of most dwarf galaxies: this would make it unlikely that the polar rings result from the recent accretion of a single gas-rich dwarf. A survey of the fields around our sample galaxies shows in all but one case the presence of at least one companion with either a similar redshift or similar blue magnitude; these companions are close enough to have encountered the polar-ring galaxy in <1 Gyr. The companion galaxies may be the source of the detected gas, through tidal stripping.

Key words: ISM: molecules – galaxies: elliptical and lenticular, cD – galaxies: formation – galaxies: interactions – galaxies: ISM – galaxies: kinematics and dynamics.

1 INTRODUCTION

Polar-ring systems are early-type (generally S0) disc galaxies surrounded by a ring almost perpendicular or highly inclined to the main stellar disc; these rings contain stars and ionized gas. It was immediately apparent from spectra that the material in the rings is rotating about the centre of the galaxy, with angular momentum vectors perpendicular to those of the main stellar body of the galaxy. This raises several questions: from where did the material in the rings come? And, is the configuration stable? The recent Polar Ring Catalogue (hereafter the PRC), compiled by Whitmore et al. (1990), includes more than 50 possible cases for study. The authors of the PRC estimate that about 5 per cent of all S0 galaxies now have a polar ring or have had one in the past.

The fact that the angular momentum vectors of the rings and the main stellar body are perpendicular to one another suggested a possible external origin for the ring material (Schweizer, Whitmore & Rubin 1983). Possible models of ring generation include the capture of a satellite galaxy (Toomre 1967) or the accretion of material between closely interacting galaxies, as described by Toomre & Toomre (1972). The basic idea is that the captured gas is drawn into a disc-like configuration, the centre of which may be depleted through cloud–cloud interactions with any pre-existing gas in the galaxy. This would leave a ring-like structure, in which new stars could form.

Once accreted, however, the gas in the polar ring may be unstable due to collisional dissipation and also because ring material at different radii precesses at different rates in the gravitational potential of the galaxy, which tends to destroy the co-planarity of the ring. The warped or multiple structure of some rings (PRC; Sparke 1986) may reflect these processes. On the other hand, some polar rings appear to be old (Whitmore et al. 1987), suggesting that some stabilizing mechanism could exist. For example, if the ring mass is relatively high, in comparison with that of the host galaxy, it might be stable through 'self-gravitation' (Sparke 1990), or the presence of a massive triaxial dark halo might stabilize the rings (Whitmore et al. 1987; Reshetnikov & Combes 1994). Alternatively, rings may take a long time to form, perhaps longer than 2.5 Gyr (Quinn 1991).

The polar-ring galaxies have recently been reclassified as spirals, rather than S0s (NGC 660 by van Driel et al. 1995, and NGC 2748 by Bettoni et al., in preparation), but given

the state of confusion over the deeper physical significance over the Hubble type we choose in this work to treat all polar-ring galaxies as coming from the same parent population.

A recent survey of H I in 47 polar-ring galaxies has been performed by Richter, Sackett & Sparke (1994; hereafter RSS); the average detected mass in atomic hydrogen is 5×10^9 $M_\odot$, very high for early-type galaxies. Unfortunately, the resolution of the observations was not sufficient to determine where most of the gas resides – it could either be in the rings, or distributed throughout the main stellar body, as in a normal galaxy. To better estimate the total mass of cold gas present in polar rings, and to provide better constraints on its location, we searched for CO emission from a sample of 10 polar-ring galaxies selected from the PRC. We detected all 10, and find that the mass of molecular gas suggested by these observations is comparable to, but less than, the H I mass.

The total mass of gas observed calls into question the view that the rings formed through the accretion of a gas-rich dwarf galaxy, because in general dwarf galaxies have insufficient gas to explain the observations.

2 OBSERVATIONS AND DATA REDUCTION

We searched for CO emission from 10 galaxies (see Table 1 for basic parameters), at the $J=1\rightarrow0$ transition ($\lambda=2.6$ mm); we observed the centre and at least two other positions on the polar ring itself. In some cases, we also searched for CO emission at other offsets along the major axis of the stellar body. The observed positions and corresponding line parameters are shown in Table 2. The images of the galaxies, extracted from the Digitized Sky Survey,[1] are shown in Fig. 1, with the beamsize and position indicated for each galaxy. When possible, we were interested not only in detecting the CO but also in estimating the quantity of H_2 and the direction of its rotation, which was possible when the gas angular momentum vectors were aligned with those of the stars.

2.1 15-m SEST telescope

The data were obtained in 1993 September 13–23 using the 3-mm cooled Schottky receiver at the Swedish-ESO-Submillimeter-wave Telescope (SEST) at La Silla, where the beamsize at 115 GHz is HPBW = 43 arcsec. We recorded both polarizations, yielding two independent spectra from the 728 channel × 0.69 MHz channel^{-1} acousto-optical spectrometers. These independent spectra were coadded during the data reduction. Typical system temperatures, on the Rayleigh–Jeans main beam temperature scale ($T_{\rm mb}$), ranged between 600 and 860 K in one polarization (Mixer A), and between 650 and 1400 K in the other one (Mixer B). We used double-beam switching, with a beam throw of 12 arcmin to produce the flattest possible baselines.

Pointing was checked every 2 to 3 h, using the SiO maser sources *o* Ceti, R Dori and R Aqr, which were the nearest reference sources in the sky to the sample galaxies. Changes in pointing offsets during the same transit were typically $\lesssim 5$ arcsec. On differing nights, the offsets for the same region of sky could change by up to ~ 10 arcsec.

The scans for each position were coadded, Hanning-smoothed, and replotted at a channel spacing of from 18 to ~ 29 km s^{-1} (depending on the strength of the signal). A linear baseline was then fitted and subtracted from the smoothed spectra. Total integration times per point ranged from 2 to 5 h. The final results are shown in Fig. 2.

Table 1. The observed galaxies. The common name is listed first, with the identification in the Polar Ring Catalogue (Whitmore et al. 1990) given immediately below. The other quantities are from Richter et al. (1994), except for: [a]this work; [b]NED; [c]Tully (1988); [d]from van Driel (private communication); [e]Bottinelli, Gouguenheim & Paturel (1982). Total blue magnitudes are from LEDS; FIR upper limits assume $S_{60} < 0.2$, $S_{100} < 1$.

Name PRC	Distance (Mpc) $v_\odot$ (km s^{-1})	S_{100} (Jy) S_{100}/S_{60}	M(HI) (10^9 $M_\odot$) $L_{\rm FIR}$ (10^9 $L_\odot$)	B_T (mag.) L_B (10^9 $L_\odot$)
IC 51	24.2	4.7	1.59	14.5
B-1	1709	2.1	2.40	1.1
ESO474-G26	211[a]	1.8[b]	-	14.57
C-3	15,800[a]	2.0[b]	97.6	112.7
A0136-0801	75.1	-	5.07	19.92
A-1	5521	-	< 1.2	1.3
NGC 660	13.9	101.5	8.52	11.79
C-13	848	1.45	21.4	7.0
UGC 1198	18.7	3.0	0.135	15.43
C-12	1149	1.2	1.31	0.5
ESO415-G26	60.5	-	5.37	14.69
A-2	4572	-	< 0.8	6.9
NGC 2748	23.8[c]	19.4[b]	4.20[e]	12.38
C-28	1391[c]	2.5[b]	8.42	14.6
UGC 5600	39.6	5.0	4.45	14.65
B-11	2769	1.4	8.59	3.8
NGC 3934	49.2	4.3	3.25	14.84
C-38	3793	1.9	9.53	4.4
ESO603-G21	43.7	2.9	6.42	15.58
B-21	3180	2.0	4.99	1.5

2.2 12-m NRAO telescope

The NRAO[2] observations were made at the 12-m telescope at Kitt Peak 1993 July 8–11. The 12-m beamsize (HPBW) is 55 arcsec at 115 GHz. The dual-polarization 3-mm SIS receivers were utilized in conjunction with the 256 channel × 2 MHz channel^{-1} filterbanks. System temperatures ranged between ~ 350 and 1450 K on the Rayleigh–Jeans main beam brightness temperature scale ($T_{\rm mb}$); most of the data were collected while system temperatures were between 400 and 700 K. The nutating subreflector was used for all observations. Telescope pointing and focus were

[1]The 102 CDROMs of the Digitized Sky Survey were produced at the Space Telescope Science Institute under US Government grant NAG W-2166.

[2]The National Radio Astronomy Observatory is operated by Associated Universities, Inc., under cooperative agreement with the National Science Foundation.

Table 2. The observed points. Centroid velocities and uncertainties (the latter from Gaussian fits) are listed only if there is sufficient signal-to-noise ratio to justify them. For IC51, the peculiar distribution of the emission renders the identification of centroids of dubious value. The position, telescope and range over which the emission was integrated retain the same values as the line above, unless a change is specifically indicated. Coordinates are at 1950.0. The positions labelled 'SUM' are the result of coadding all the data at all points in the galaxy. This is an effective way of identifying weak emission (which is true for almost all of the observed galaxies).

Name	α δ	$\Delta\alpha$ ($''$)	$\Delta\delta$ ($''$)	Telescope	Range (km s^{-1})	I_{CO} (T_{mb} km s^{-1})	v_{cen} (km s^{-1})
IC 51	$0^h43^m53.6^s$	SUM		NRAO	1484 to 1905	0.88±0.44	1675±32
	-13°42'56"				1296 to 2155	3.24±0.65	1726±32
		0	0		1276 to 2176	3.5±1.2	1675±45
					1482 to 1905	1.27±0.74	1823±62
		-10	-12		1541 to 1908	1.38±0.55	1858±6
					1541 to 2117	2.57±0.63	?
					1300 to 2114	3.45±0.82	?
		10	12		1651 to 1843	0.37±0.26	1726±8
					1300 to 2152	2.60±0.69	?
					1300 to 1853	2.00±0.41	?
ESO474-G26	$0^h44^m40.0^s$	SUM		SEST	15630 to 16000	1.79±0.19	15794±11
	-24°38'36"	0	0			2.25±0.21	15802±12
		0	-21			2.30±0.29	15762±18
		0	21			0.86±0.36	15840±28
A0136-0801	$1^h36^m25.4^s$	SUM		SEST	5185 to 5811	1.06±0.26	5390±60
	-8°01'14"	0	0			1.57±0.59	5500±130
		15	12			1.01±0.43	5400±150
		-15	-12		5248 to 5523	0.64±0.31	5420±30
NGC 660	$1^h40^m20.7^s$	0	200	NRAO	650 to 900	0.62[a]±0.51	820±13
	13°23'32"	10	200			0.84±0.59	794?
		-10	200			0.32±0.48	824?
		25	100		680 to 830	1.66±0.35	764±7
		-25	-100		800 to 990	0.34±0.45	?
		-30	50		700 to 970	1.52±0.60	830±20
		30	-50		815 to 1095	2.99±0.66	983±13
UGC 1198	$1^h40^m54.1^s$	SUM		NRAO	1085 to 1235	0.57±0.12	1172±8
	85°00'35"	0	0			0.41±0.22	
		0	-15			0.62±0.17	1167±13
		0	15			0.77±0.22	1189±5
ESO415-G26	$2^h26^m12.0^s$	SUM		SEST	4194 to 5243	2.45±0.30	4629±44
	-32°06'18"	0	0		4250 to 4922	1.31±0.30	4506±77
		-10	0			2.39±0.40	4590±57
		10	0		4272 to 5243	3.60±0.57	5097±71
NGC 2748	$9^h08^m02.6^s$	SUM		NRAO	1320 to 1635	2.44±0.21	1482±8
	76°40'53"	0	0		1335 to 1620	4.13±0.41	1453±11
		-20	-20		1410 to 1655	3.34±0.45	1535±12
		-20	20		1300 to 1650	0.54±0.35	1468±37
		20	-20		1320 to 1635	3.37±0.32	1495±9
		20	20		1320 to 1580	2.26±0.51	1401±15
UGC 5600	$10^h19^m17.4^s$	SUM		NRAO	2645 to 2815	0.76±0.12	2743±7
	78°52'48"	0	0			0.76±0.21	2746±15
		14	0		2680 to 2815	0.84±0.22	2738±11
		-14	0		2600 to 2815	1.34±0.26	2714±21
NGC 3934	$11^h49^m37.4^s$	SUM		NRAO	3405 to 3900	1.67±0.15	3666±19
	17°07'50"	0	0		3417 to 3900	1.94±0.21	3676±13
		13	-5		3421 to 3900	2.20±0.32	3587±16
		-13	5		3405 to 3900	1.91±0.30	3693±16
		-9	-11		3443 to 3900	1.74±0.29	3791±35
		9	11		3443 to 3844	1.28±0.27	3706±18
ESO603-G21	$22^h48^m41.0^s$	SUM		NRAO+SEST	2965 to 3310	1.61±0.20	3125±13
	-20°30'42"	0	0	SEST	2991 to 3281	1.61±0.29	3124±16
		-13	4	NRAO	2965 to 3310	1.94±0.44	3070±34
					2963 to 3152	1.46±0.29	3070±24
		13	-4		2983 to 3374	2.66±0.39	3144±23
					3049 to 3315	1.84±0.34	3272±24

[a]Sum of (−10, 200), (+10, 200).

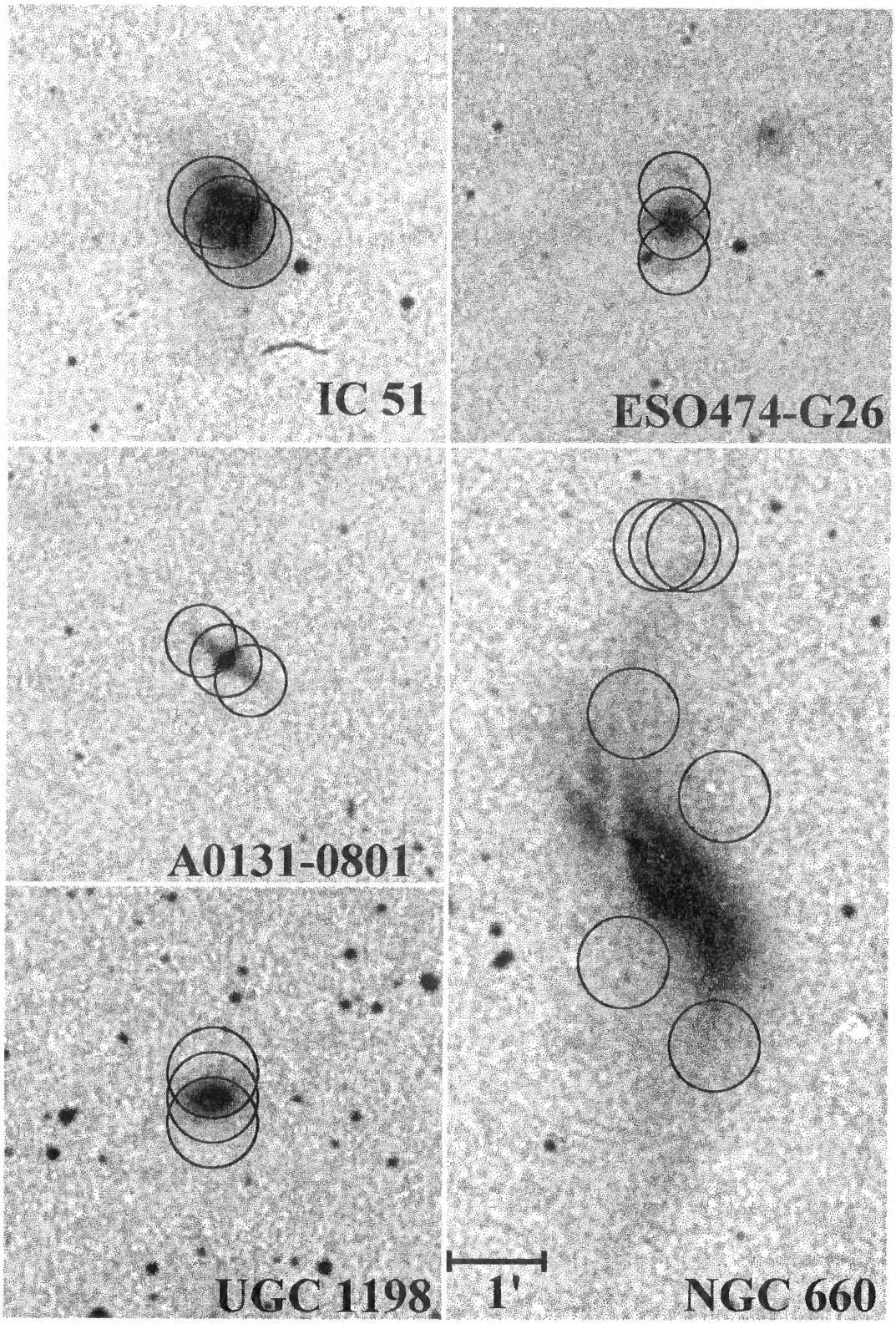

Figure 1. Images of our program galaxies from the Digitized Sky Survey, with the beam of the various CO observations indicated by circles. North is at the top and east at the left. The scale, indicated by the horizontal bar (1 arcmin), is the same for all of the images.

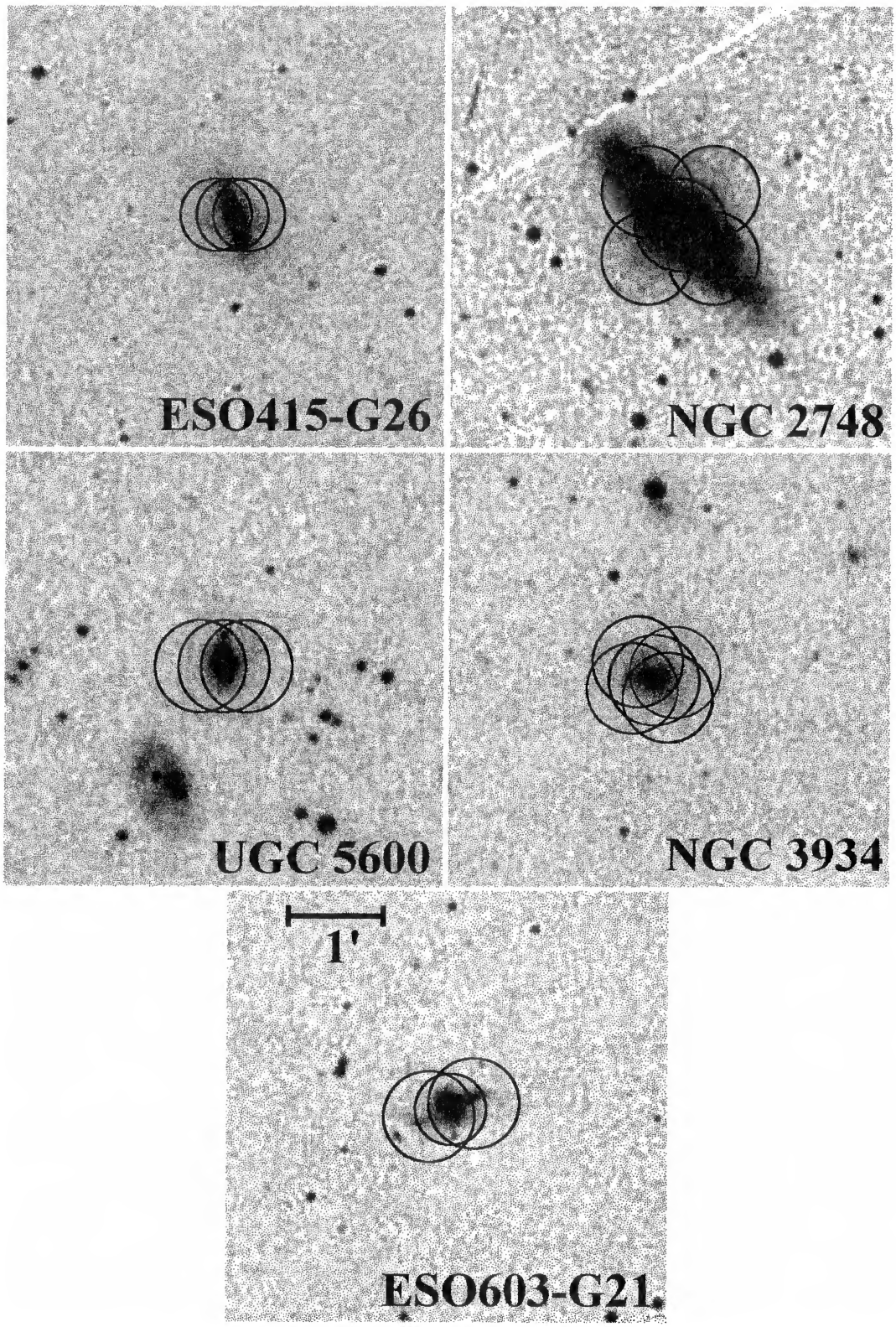

Figure 1 – *continued*

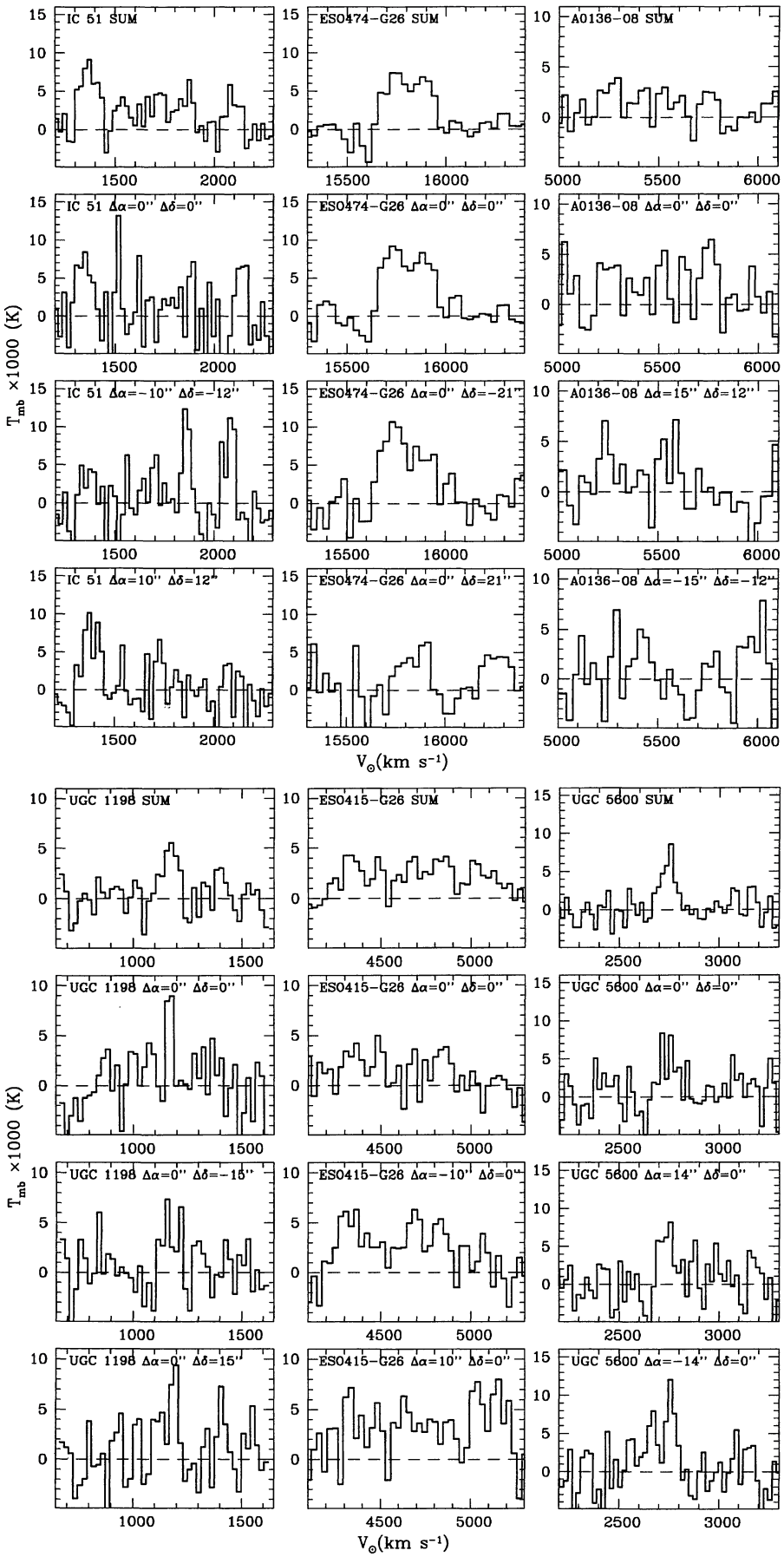

Figure 2. The smoothed and baseline-subtracted spectra. The dashed line indicates the baseline.

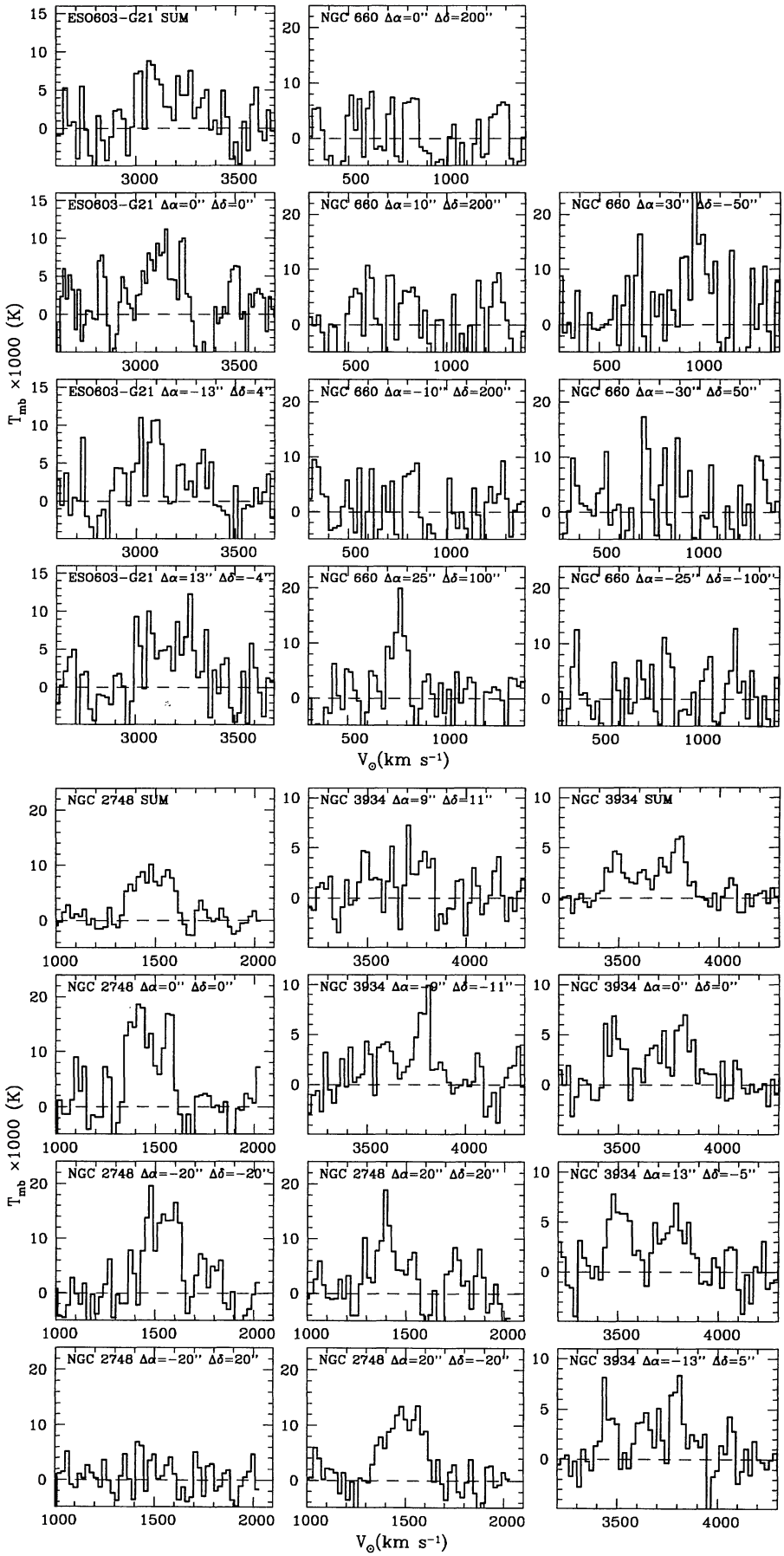

Figure 2 – *continued*

checked every 3 to 4 h. The typical uncertainty in pointing the 12-m telescope is ~7 arcsec.

3 RESULTS

We give here a short description of the results for each galaxy, and mention any other data that will be useful for the discussion which follows. The identification number of each galaxy in the PRC is indicated in parentheses.

Except for NGC 2748, the total molecular hydrogen masses were calculated (for simplicity of comparison with other samples) from the spectra indicated as 'sum' in Fig. 1 and Table 2, using a beamsize representative of the area covered by the observations. For simplicity, we have adopted the distances listed by RSS, except for two galaxies not observed in that study: for ESO 474-G26, we used the distance from the redshift ($H_0 = 75$ km s^{-1} Mpc^{-1}), applying the flux correction factor $(1+z)^{-4}$ (this is the only case where the cosmological correction was applied), and for NGC 2748 we used the distance given by Tully (1988). Our systematic velocities are taken from the PRC. The H_2 masses assume the 'standard' conversion factor found from the calibration applied to Galactic molecular clouds: $N(H_2) = 3 \times 10^{20} I_{CO}$ molecules (K km s^{-1})$^{-1}$ (Solomon et al. 1987). While this factor may well be wrong for these galaxies, since the physical conditions in the molecular clouds in polar rings are completely unknown, in the absence of any other information we have selected this value for ease of comparison with other galaxies. It could be argued that the gas temperature will be higher in the rings than in the disc of the Milky Way; if so, this technique will overestimate the mass. On the other hand, if the metallicity of the gas is lower than in the Milky Way, as it might be if the gas came from a dwarf or relatively unevolved system, a standard conversion factor will underestimate the mass. The fact that the molecular masses so determined are rather less than the H I masses – unlike normal early-type galaxies – may indicate that we are underestimating, rather than overestimating, the mass.

3.1 IC 51 (B-1)

We find a redshift $cz = 1666$ km s^{-1} for this galaxy, also known as Arp 230. It appears to be a merger remnant (PRC); stellar shells are visible in the NE–SW direction. A companion galaxy of similar size, PGC 2496, is separated from it by 76 arcmin (~535 kpc) in the plane of the sky; the difference in systemic velocities is 90 km s^{-1}. The ring and stellar components of IC 51 have about the same size; the telescope beam covers most of the galaxy in the central pointing. Our observations are slightly noisy, but some peaks are apparent at the nucleus and in the offset pointings. They are at ~1380 and ~1725 km s^{-1} north-east; ~1860 and ~2080 at south-west. H I observations made with the VLA (Schiminovich, private communication) found emission only around 1725 km s^{-1}, although a recent H I spectrum obtained by van Driel (private communication), using the Nancay telescope, shows strong emission in the range 1310–1650 km s^{-1}, with a minor peak at 1725, and possible emission in the range 1800–1900 km s^{-1}. (The discrepancies between the H I observations have not yet been resolved.) Even more surprisingly, the atomic gas seen by the VLA on the north-west side is apparently approaching, opposite to the CO. We have at present no explanation for this disagreement.

We initially discounted the additional CO peaks as noise, because of the inconsistency with the VLA H I data (although they are themselves discrepant with the Nancay data). After we found three other cases with CO emission not coincident in velocity space with the H I, however, and after carefully re-examining the raw data, we feel that these CO peaks may well be real. In future observations this point will be checked. If we accept that we are seeing CO in these additional peaks then something very unusual is happening in IC51. Looking at a 2.2-m ESO telescope image (Carollo, private communication), it seems that the morphology of IC51 is more similar to that of a distorted, many-rings system such as NGC 660, rather than a 'classical' polar-ring galaxy (e.g. NGC 4650A). It is possible that the atomic and molecular components of the gas have different velocities, perhaps denoting very different spatial locations. We cannot draw any definite conclusions at this time, because of the peculiar nature of this system.

The molecular hydrogen mass was determined assuming an effective beam area of 1.15 arcmin^2; we estimate that ~80 per cent of that mass lies in the ring structure, assuming that the prominent features at 1350 and 2100 km s^{-1} are associated with the ring.

3.2 ESO 474-G26 (C-3)

This galaxy has a nucleus surrounded by two perpendicular, irregular rings. Optical spectra (PRC) indicate that the ionized gas rotates, with the north and west sides receding. No H I observations are available because of the high redshift. We see a relatively strong CO signal; it is clearly visible in the 5-h integration on the nucleus. The CO velocity is ~15 800 km s^{-1}, about 400 km s^{-1} less than that for the optical data, a typical level of agreement for redshifts of this order. The southern pointing – (0, −21 arcsec) – has a strong peak at 15 750 km s^{-1}, near the lower range of velocities detected in the nucleus, while the northern offset – (0, 21 arcsec) – has stronger emission at higher velocities, suggesting that the outer (north–south) ring has the northern side receding. This agrees with the optical data; the molecular gas appears to rotate in the same direction as the ionized gas.

The molecular hydrogen mass was determined assuming an effective beam area of 1.15 arcmin^2. About half of the H_2 seems to be associated with the rings.

The field around this galaxy does not show any object of similar magnitude or size within 11 arcmin, or 675 kpc, the distance covered in 1 Gyr by a galaxy moving in a direction perpendicular to the line of sight at a velocity of 600 km s^{-1}. The closest object of comparable magnitude ($B_T = 16$) is IC 1852, lying at 13 arcmin north-west. Very close to ESO 474-G26 there is, however, a fainter galaxy of unknown redshift.

3.3 Anon 0136 – 0801 (A-1)

This is one of the best known cases of a polar-ring galaxy but, unfortunately, it is quite small on the sky, so the SEST beam covers as much as 80 per cent of the galaxy. The north-east and south-west offsets, 19 arcsec from the

nucleus, give similar results: a very faint signal seems to be present, but the integration time (2 h per pointing) is too short to claim a first detection or to determine the sense of rotation. The sum of all the data does show, however, CO emission at the 4σ level. Previous observations of optical emission lines by Schweizer et al. (1983) indicate a velocity of $\sim$5680 km s^{-1} on the north-east side of the ring and $\sim$5380 km s^{-1} on the south-west side; the galaxy has a systemic velocity of 5528 km s^{-1}. The H I data (van Gorkom, Schechter & Kristian 1987) show the same trend. In our data for the south-west position, a peak appears near the optical velocity, but its significance is very low. In the summed data features are visible at velocities (5250 km s^{-1}) lower than those of the H I. The molecular hydrogen mass was determined assuming an effective beam area of 0.75 arcmin^2.

There is a larger galaxy, PGC 6186, 24 arcmin distant ($\sim$519 kpc) from A0136 − 0801; their redshifts differ by 31 km s^{-1}.

3.4 NGC 660 (C-13)

This edge-on galaxy has multiple, inclined rings making an 'integral' sign on the sky. Its systemic velocity is 852 km s^{-1}. It has been studied at 21 cm by Gottesman & Mahon (1990), who produced a detailed rotational picture of the central body and the major axis of the outermost ring. A kinematical model of the complex H I velocity field has been produced by Arnaboldi & Galletta (1993). The field around it contains three objects of similar redshift (within 80 km s^{-1}); two of them, UGC 1195 and 1200, are aligned with the outer ring direction and lie at distances of 22 and 29 arcmin ($\sim$89 and $\sim$117 kpc) respectively.

CO emission from the rings was detected by Combes et al. (1992). H I emission is strongest at velocities between 780 and 840 km s^{-1}, while the CO is brighter between 700 and 760 km s^{-1} (Combes et al. 1992). This asymmetry is similar to that found in the SB0 galaxy NGC 4546 by Sage & Galletta (1994). On the basis of a detailed investigation, van Driel et al. (1995) concluded that NGC 660 is a spiral galaxy whose ring is sustained by self-gravity.

NGC 660 is so big in the sky that we observed only a few points on the rings. We detected CO at three positions: (30 arcsec, −50 arcsec), (−30 arcsec, 50 arcsec) and (25 arcsec, 100 arcsec). The velocities of the CO lines agree with those of the H I at the last position only; the wide peak between 900 and 1100 km s^{-1} at the (30 arcsec, −50 arcsec) position is $\sim$130 km s^{-1} higher than the 21-cm emission. Of course, the atomic and molecular gas may be in very different spatial locations, yet still along the same line of sight. We suggest that the H I and CO data indicate a complex of rings with different velocities, with the north side of the galaxy approaching.

Based on the observations of CO emission from the rings (Combes et al. 1992; this work), and comparison with larger scale studies of the entire galaxy (Solomon & Sage 1988), we estimate that $\sim$10 per cent of the total molecular mass associated with the galaxy lies within the rings.

3.5 UGC 1198 (C-12)

Also known as VII Zw 3, this is a small galaxy, lying almost east–west in the sky, which is crossed in the north–south direction by a slight enhancement of optical light. The telescope beam (55 arcsec) at the centre position includes most of the galaxy and the presumed polar ring. A narrow CO feature appears at a velocity $\sim$1170 km s^{-1}. The signal increases at the northern offset (+15 arcsec) and becomes lower and broader at the southern offset (−15 arcsec); the two integrated intensities are the same, within the uncertainties of the measurements, but the CO emission may follow the trend indicated by the light of the possible polar ring, which is described as brighter in the northern side (PRC). The molecular hydrogen mass was determined assuming an effective beam area of 0.9 arcmin^2.

Four objects of comparable (15–16) magnitude but unknown redshift lie in the field of UGC 1198. The closest one, PGC 8169, is 24 arcmin ($\sim$130 kpc) away, while PGC 9563, 94 arcmin ($\sim$511 kpc) away, is the most distant.

3.6 ESO 415-G26 (A-2)

This is a well-known and well-studied polar-ring galaxy, also known as MCG-5-7-1. Unlike Anon 0136 − 0801 (A-1), its polar ring in the optical images is less extended than the stellar disc. The H I (van Gorkom et al. 1987) and optical (Whitmore et al. 1987) emission line velocities agree in amplitude and direction, with the west side of the ring approaching at a relative velocity of $\sim$200 km s^{-1}. The relative velocity of the optical emission lines on the eastern side is similar to that, but the atomic gas is receding at only 150 km s^{-1}. As with Anon 0136 − 0801, the well-defined polar ring does not show a strong CO signal. A broad feature appears in all three SEST pointings: the central position includes the whole ring, which has a spatial extent of <40 arcsec, and therefore may include gas at different velocities. From our data it is hard to say if we have identified the direction of rotation. The signal at $v\sim5100$ km s^{-1} at the eastern position agrees with the sense of rotation of the H I and optical emission lines, but exceeds their relative shifts considerably. the molecular hydrogen mass was determined assuming an effective beam area of 0.7 arcmin^2. About 60 per cent of the molecular gas is associated with the rings, assuming that the features at 4300 and 5100 km s^{-1} arise in the rings themselves.

ESO415-G26 has a smaller companion, PGC 9331, which lies 18 arcmin ($\sim$310 kpc) distant, with a redshift that differs by 52 km s^{-1}.

3.7 MGC 2748 (C-28)

NGC 2748 has a systemic velocity of 1476 km s^{-1}, and exhibits a faint structure perpendicular to the stellar disc. A detailed kinematical and photometrical study of this object indicates that it is a spiral galaxy surrounded by a polar ring (Bettoni et al. 1996), perhaps similar to NGC 660, although of a later type. The area around it contains many galaxies of unknown redshifts and one faint object, PGC 26654, at the same redshift and 38 arcmin distant, which corresponds to a projected distance of 261 kpc.

A double-horn-like CO signal appears in the nucleus, with maxima at 1400 and 1550 km s^{-1}. Moving along the galaxy major axis, there is CO emission at 28 arcsec north-east (peak at 1395 km s^{-1}) and at 28 arcsec south-west of the

nucleus, with the latter being broader and stronger for velocities $\sim$1500 km s^{-1}. The faint optical ring also presents a clear CO signal, centred at $\sim$1500 km s^{-1}, at 28 arcsec south-east. The spectra are noisy and the signal fades out at 42 arcsec south-east, and on the other side of the ring at 28 arcsec north-west. The CO emission seems asymmetric, with the southern part receding. The molecular hydrogen mass was determined by simply adding the observed integrated intensities, with the exception of the ($-$20 arcsec, 20 arcsec) position. Assuming that the centre position we used is correct, $\sim$25 per cent of the molecular mass is in the ring.

3.8 UGC 5600 (B-11)

This system appears morphologically complex; it is interacting with a close companion (UGC 5609) of similar size that lies only 1 arcmin ($\sim$14 kpc) away. Two other companions of similar redshift are also nearby. Because of the interaction, it does not have a typical polar-ring morphology. A thin extension, perhaps an edge-on inner ring, appears in the north–south direction, while an outer ring, with the same orientation but rounder (maybe less inclined with repect to the sky) surrounds the galaxy. Our observations include most of the above structures, and CO appears to be present in all but one of the pointings. The nuclear emission peaks at about 2750 km s^{-1}, in agreement with the systemic velocity (2765 km s^{-1}) determined from the optical emission lines. A peak centred at a similar velocity appears at 14 arcsec north, while a noisier peak appears at 14 arcsec south, perhaps with some emission at velocities lower than systemic. The molecular hydrogen mass was determined assuming an effective beam area of 0.9 arcmin^2.

3.9 NGC 3934

NGC 3934 has an X-shaped structure; the large-scale images published in the PRC indicate a dark ring running approximately NW–SE. The presence of shells in deeper images and a blend between many different structures indicates the possibility of a past merger, instead of an independent ring that is inclined with respect to the plane of the galaxy. There is one companion, NGC 3433, at the same redshift (and having a similar magnitude and size) about 4 arcmin ($\sim$57 kpc) away.

We have detected CO at all five observed positions; the interior X-shaped structure is included in all the pointings because of the small size of the galaxy on the sky. Two ranges of velocities are apparent from the data: a large peak at about 3450 km s^{-1}, which is more evident at (13 arcsec, $-$15 arcsec) (on the dark ring), and a similar peak at about 3800 km s^{-1}, which is stronger to the south-west (along the presumed major axis of the stellar body). The other side of the ring, which is smoother in the optical images, shows fainter CO emission. We deduce that the gas motions are quite complex, but we do not have the spatial resolution to interpret the data unambiguously. The multiple peaks in the CO data are reminiscent of the NGC 3690 + IC 694 system (Solomon & Sage 1988), which consists of two interacting galaxies. Although the CO spectra do not agree – at first glance – with the H I spectrum reported by RSS, there is some evidence in the latter spectrum for the features seen here. In particular, note the strong dip in the H I spectrum at $\sim$3600 km s^{-1}, which is quite evident in the CO data. There may also be H I emission extending down to $\sim$3400 km s^{-1}, as is evident in the CO spectra; a different baselining of the H I data might bring such a feature to more prominence.

The molecular hydrogen mass was determined assuming an effective beam area of 1.25 arcmin^2. If the CO peaks at about 3500 and 3800 km s^{-1} arise from gas within the ring, then $\sim$80 per cent of the molecular gas resides there. The narrow H I line could then suggest that atomic gas dominates within the galaxy, with the molecular material in the ring.

3.10 ESO 603-G21 (B-21)

This galaxy has a recession velocity of 3150 km s^{-1}, and in large-scale images exhibits a warped ring, which appears dark when crossing the stellar body (PRC). It is surrounded by a number of very faint objects, visible as condensation of luminous matter (see PRC, fig. 3f). Three close galaxies have a similar redshift (within 75 km s^{-1}), and the closest one, ESO 603-G20, is one magnitude brighter than ESO 603-G21 and lies only 5 arcmin distant ($\sim$64 kpc). It is a very narrow, straight and knotted object, almost aligned toward ESO 603-G21.

The optical emission-line rotation curve of the ring (PRC) indicates a maximum relative velocity of 240 km s^{-1}, with the south-east side receding. The SEST data indicate the presence of CO between 2950 and 3250 km s^{-1}, in agreement with the ionized gas. The offset pointings made at the 12-m telescope suggest a possible feature near 3100 km s^{-1} to the north-west. If this feature is real, it is in agreement with the motion of the ionized gas. The molecular hydrogen mass in Table 3 was determined assuming an effective beam area of 0.9 arcmin^2.

4 DISCUSSION AND CONCLUSIONS

Our results are summarized in Table 3, where we list the H_2 masses found for the observed galaxies, along with those for similar cases from the literature. H I masses and far-infrared (FIR) luminosities are from RSS, except as indicated. In the case of NGC 5128 (Cen A), the M_{H_2} has been scaled to the distance of 3.3 Mpc used by RSS, and their value of M_{H_I} has been quoted. The M_{H_I} of NGC 2748 is derived from the 21-cm flux listed by Bottinelli et al. (1982).

4.1 CO properties in the observed polar-ring systems

Galaxies in the PRC are separated into classes according to the regularity ('goodness') of the appearance of the polar rings, and according to the kinematical confirmation of the polar-ring rotation. We have observed objects across the range of categories from A – definite polar rings – to C, which are possible polar-ring candidates. Looking at the data of Tables 2 and 3, we have not found any reliable relationship between the 'goodness' of the polar ring and the properties of the gas, except that (as noted by RSS) the A galaxies are often weak or undetected in the far-infrared. As a result, we believe that the classes do not correspond to different types of galaxies but rather to different evolution-

Table 3. Masses and luminosities. Gas masses and luminosities for the observed galaxies and similar cases from the literature.

Name	M_{H_2} (10^8 $M_\odot$)	$\frac{M_{H_2}}{M_{HI}}$	$\frac{L_{FIR}}{M_{H_2}}$ ($L_\odot/M_\odot$)	$\frac{M_{H_2+HI}}{L_B}$ ($M_\odot/L_\odot$)
Polar ring systems				
IC 51	8.9±1.8	0.56	2.7	2.25
ESO474-G26	200±20		4.9	>0.18
A0136-0801	18±4	0.36	<0.7	5.23
NGC 660	14[a]	0.16	15	1.46
UGC 1198	0.73±0.15	0.54	18	0.40
ESO415-G26	24±3	0.45	<0.3	1.12
NGC 2685	3.9[b]	0.39	0.38	0.27
NGC 2748	20±6	0.48[e]	4.2	0.42
UGC 5600	4.4±0.7	0.099	19.5	1.29
NGC 3934	21±2	0.65	4.5	1.20
NGC 4650A	8[b]	0.31[c]	<1[b]	0.52
ESO603-G21	11±1	0.17	4.5	5.07
Minor-axis dust-lane galaxies				
NGC 1316[d]	9.5	>4.8	4.1	
NGC 1947[d]	4.2		1.8	
NGC 5128[d]	6.1	1.0	26	
NGC 5363[d]	2.9	1.3	5.9	
NGC 5266[d]	24	0.16	3.4	

[a]From Solomon & Sage (1988);
[b]from Watson et al. (1994);
[c]from van Gorkom et al. (1987);
[d]from Sage & Galletta (1993) and references therein;
[e]from Bottinelli et al. (1982).

ary stages, with the most regular rings being the oldest and the most irregular the youngest.

We have been able to determine, at least in some cases, that there is molecular gas in the rings. The shapes of the line profiles (which are in general centrally peaked) suggests that molecular gas also exists in the main stellar body of the galaxy.

One of the most puzzling results is that in four out of 10 cases the CO emission covers a wider range of velocities than the H I and/or optical emission lines (in the case of IC 51, the direction of motion of the H I gas disagrees with that of the H_2). It may be that in some cases there are multiple ring structures with different phases of gas, but this seems evident only for NGC 660. We remember that in another case of a gas-accreting galaxy – NGC 4546: Sage & Galletta (1994) – the molecular and the atomic gas dominate in distinct regions inside the galaxy and appear in different velocity ranges.

Several results are, however, immediately apparent from the data. The H_2 masses typically range between 10^8 and 10^9 $M_\odot$; this is a lot of gas for early-type galaxies. The only exception (on the low end) is the dwarf galaxy UGC 1198: its blue luminosity is 5×10^8 $L_\odot$, about the same as the Small Magellanic Cloud. It does, however, have a large gas mass for its size and type. At the opposite extreme, for ESO474-G26 the H_2 mass is 2×10^{10} $M_\odot$ – as much as a giant spiral galaxy – in agreement with its large optical luminosity, 10^{11} $L_\odot$. No H I data are available for this galaxy and therefore the total mass of cold gas will be even higher.

The ratio of molecular to atomic mass is always lower than unity, unlike normal spiral galaxies (e.g. Sage 1993) and dust-lane ellipticals (Sage & Galletta 1993); this quantity varies over a wide range, but seems uncorrelated with other parameters. As above, this might be expected on physical grounds if the gas resulted from an interaction/capture event, in which case much of the H_2 might be heated sufficiently (probably by shocks) to dissociate the molecules. On the other hand, it might indicate that we are systematically *underestimating* the total molecular mass, perhaps because the ring gas has low metallicity.

The ratio of gas mass to luminosity, M_{H_2+HI}/L_B, is higher than expected for S0s or early-type spirals, and in some cases is bigger than the average value for late-type spirals (Sage 1993) and irregulars (Sage et al. 1992), confirming the conclusions reached by RSS. The radio M_{H_2+HI}/L_B for the rings taken alone would be even higher, suggesting that they have turned relatively little of their gas into stars, perhaps because so little of the gas is in molecular form. (It is generally thought that the gas must be in molecular form to cool sufficiently to form stars.)

The average ratio of FIR luminosity to molecular gas mass for those members of our sample that were detected by *IRAS* is $\langle L_{FIR}/M_{H_2} \rangle = 7.5 \pm 2.3$, slightly more than twice the average for a distance-limited sample of normal spiral galaxies (Sage 1993). The relationship between the H_2 mass and the FIR luminosity is generally attributed to the causal relationship between the number of massive young stars and the gas available to make more stars. What is particularly interesting is the large spread in this ratio: the galaxies with the most regular rings (A0126 – 0801, ESO 415-G26, NGC 4650A) are systematically weak in FIR emission (as already noted by RSS), but still have detectable, albeit weak, CO emission.

4.2 Comparison with minor-axis dust-lane ellipticals

In Table 3 we list comparison data for five minor-axis dust-lane ellipticals, from Sage & Galletta (1993). These galaxies (Bertola & Galletta 1978) probably represent the elliptical galaxy equivalent of the polar-ring S0s: both classes possess rings of gas crossing the galaxies perpendicular to their major axes and are interpreted as the result of the accretion of gas from the environment. All the minor-axis dust-lane ellipticals surveyed in CO showed emission along the ring or disc, perpendicular to the galaxy plane. The molecular gas moves in the same directions as the ionized gas, and with comparable velocities (Sage & Galletta 1993). Some of them are listed in the PRC in Category D (related objects) but differences in the properties of the accreted gas do exist. Elliptical galaxies with dust-lanes sometimes have a disc instead of a ring; polar-ring galaxies always lack of the inner part of the perpendicular gas distribution. On the other hand, the H_2 masses observed in polar-ring galaxies are comparable to those detected in the minor-axis dust-lane ellipticals. In both classes, there is substantially more molecular hydrogen than in the average S0 or elliptical galaxy. This is expected if the gas is accreted, as accretion is independent of the galaxy morphology.

4.3 Origin of the accreted gas

The gas content of polar-ring galaxies appears to be rather different from normal early-type systems. If, as seems

reasonable, much of the gas now in these galaxies was accreted long after the initial epoch of galaxy formation, the properties of the gas would probably reflect that accretion event rather than the initial properties of the galaxy itself. It is also reasonable to expect some interaction between the accreted material and any pre-existing gas, which may explain some of the differences between the galaxies. For example, if part of the observed gas was pre-existing (e.g. the gas detected in the main stellar body of NGC 2748 and 3934), and part was accreted, this might give the galaxy a higher $M_{H_2+H\,I}/L_B$ ratio than expected, and account for a wide spread of the properties involving the gas.

One possible explanation for polar-ring structure discussed in the literature is the capture and disruption of a gas-rich satellite, which has been smeared into a ring (Quinn 1991). The problem with this hypothesis is that most present-day extreme-late-type galaxies simply have insufficient gas to explain the observations reported here and by RSS – see Matthews & Gallagher (1996). The amounts of atomic and molecular gas exceed the gas content even of an average spiral (Sage 1993). Infalling gas clouds with masses of up to $10^8\,M_\odot$ have been detected around some spirals (Kamphuis 1993) and could be sources of accreted matter, but are also too small by almost an order of magnitude. While the capture of multiple gas-rich dwarfs could explain the observed quantity of gas, it seems likely that subsequent captures would disrupt a pre-existing polar ring.

However, the mass of gas that we find to be present suggests that the polar rings can be stabilized through self-gravity (e.g. Sparke 1986); if the ring is stable – or in equilibrium – for a long time, the process that generated it may have taken place in the early phase of the life of the galaxy, with no other signs of interaction remaining. At these earlier times, before substantial star formation had taken place, present-day extreme-late-type galaxies would have been about twice as gas-rich, perhaps resembling the galaxy H I 1225 + 0152, which has $M_{H\,I}/L_B \approx 10$ (Salzer et al. 1991). The largest of these dwarfs might then have supplied enough gas to form the polar rings.

Another hypothesis is the tidal stripping of gas from a massive companion, illustrated by the polar ring of NGC 6285, which is interacting with NGC 6286 (see PRC). If the polar ring is quite old, the 'donor' galaxy may now be quite far from the 'acceptor' galaxy. The required large companion should prove easy to detect. All the galaxies in our sample except ESO 474-G26 possess an apparent companion of similar size or blue magnitude within 500 kpc on the sky. A faint object is visible, however, very close to ESO 474-G26, but we have no indication about its redshift and magnitude. The differences in the redshifts of most of the presumed companions are generally no greater than 100 km s^{-1}. It is therefore possible that the observed galaxies have at least one companion with which they have interacted and have acquired their rings by stripping gas from that companion, perhaps similar to the process observed in the M81 group of galaxies (Yun et al. 1994).

ACKNOWLEDGMENTS

We have made use of the Lyon–Meudon Extragalactic Database (LEDA) supplied by the LEDA team at the CRAL-Observatoire de Lyon (France) and of the NASA/IPAC Extragalactic Database (NED), which is operated by the Jet Propulsion Laboratory, Caltech, under contract with the National Aeronautics and Space Administration. The images of the galaxies were extracted by means of the internet page SKyEye of the Bologna Institute of Radioastronomy (http://terra.bo.cnr.it/ira/skyeye). One of the authors (GG) has made use of funds of the Ministero dell'Università e della Ricerca Scientifica e Technologica, ex quota 40%, and LSS acknowledges partial support from the US National Science Foundation under grant AST-93-20403. These observations were partially based on observations made at the European Southern Observatory, La Silla, Chile.

REFERENCES

Arnaboldi M., Galletta G., 1993, A&A, 268, 411
Bertola F., Galletta G., 1978, ApJ, 226, L115
Bottinelli L., Gouguenheim L., Paturel G., 1982, A&AS, 47, 171
Combes F., Braine J., Casoli F., Gerin M., van Driel W., 1992, A&A, 259, L65
Gottesman S. T., Mahon M. E., 1990, in Sulentic J. W., Keel W. C., Telesco C. M., eds, Pro . IAU Colloq. 124, Paired and interacting galaxies. Kluwer, Dordrecht, p. 209
Kamphuis J., 1993, PhD thesis, Univ. of Groningen
Matthews L. D., Gallagher J. S., 1996, AJ, 111, 1098
Quinn T., 1991, in Casertano S., Sackett P., Briggs F., eds, Warped disks and inclined rings around galaxies. Cambridge Univ. Press, Cambridge, p. 143
Reshernikov V. P., Combes F., 1994, A&A, 291, 57
Richter O.-G., Sackett P. D., Sparke L. S., 1994, AJ, 107, 99 (RSS)
Sage L. J., 1993, A&A, 272, 123
Sage L. J., Galletta G., 1993, ApJ, 419, 544
Sage L. J., Galletta G., 1994, AJ, 108, 1633
Sage L. J., Salzer J. J., Loose H.-H., Henkel C., 1992, A&A, 265, 19
Salzer J. J., di Serego Alighieri S., Matteucci F., Giovanelli R., Haynes M. P., 1991, AJ, 101, 1258
Schweizer F., Whitmore B. C., Rubin V. C., 1983, AJ, 88, 909
Solomon P. M., Sage L. J., 1988, ApJ, 334, 613
Solomon P. M., Rivolo A. R., Barrett J. W., Yahil A., 1987, ApJ, 319, 730
Sparke L. S., 1986, MNRAS, 219, 657
Sparke L. S., 1990, in Wielen R., ed., Dynamics and Interaction of Galaxies. Springer, Berlin, p. 338
Toomre A., 1967, in Tinsley B. M., Larson R. B., eds, The Evolution of Galaxies and Stellar Populations. Yale Univ. Observatory, New Haven, p. 418
Toomre A., Toomre J., 1972, ApJ, 178, 623
Tully R. B., 1988, Nearby Galaxies Catalog, Cambridge Univ. Press, Cambridge
van Driel W. et al., 1995, AJ, 109, 942
van Gorkom J. H., Schechter P. L., Kristian J., 1987, ApJ, 324, 457
Watson D. M., Gutpill M. T., Buchholz L. M., 1994, ApJ, 420, L21
Whitmore B. C., McElroy D. B., Schweizer F., 1987, ApJ, 314, 439
Whitmore B. C., Lucas R. A., McElroy D. B., Steiman-Cameron T. Y., Sackett P. D., Olling R. P., 1990, AJ, 100, 1489 (PRC)
Yun M. S., Ho P. T. P., Lo K. Y., 1994, Nat, 372, 530